NCE Journal of Science and Engineering (NJSE), Vol. 2, June 2025 ISSN: 2717-4794

Analysis and Comparison of Unmanned Aerial Vehicle's Propellers for High Altitude Search and Rescue Missions

Sajan Bhujel[1,*], Prahar Basnet[1], Tirtha Bahadur Khadka[1], Tulsi Ram Bhandari[1], Vikash Verma[1], Chiranjivi Dahal[1]

[1]Department of Mechanical and Automobile Engineering, IOE - Pashchimanchal Campus, Tribhuvan University, Pokhara, Nepal
[*]Correspondence: pas076bme035@wrc.edu.np
Manuscript received June 7, 2021; revised January 29, 2025; accepted April 18, 2025

***Abstract*—The commercially available unmanned aerial vehicles are not good enough for search and rescue flight at high altitudes because as the altitude increases, the density of air decreases that decreases the thrust generation of the UAV. The objective of this research work is to analyse and compare the two different airfoils; Clark Y and S1223 at different altitude levels. It also focuses on increasing the efficiency of the propellers by using the aerodynamic property. SOLIDWORKS, ANSYS and Xflr5 were used for the design, simulation, and analysis of the UAV propellers and testing of its performance. Factors such as air density and angle of attack were examined to determine an efficient propeller. By using user-friendly aerodynamic inputs in the blade element theory-based design, desired output was obtained. Experimental analysis of the blade gave a thrust of 0.63N and 0.42N for S1223 and Clark Y airfoil respectively at 3000 RPM at the altitude of 3610 m. The analytical solution for thrust with the same conditions were 1.45N and 0.6N for S1223 and Clark Y airfoil respectively. The validation of experimental results had been done by the CFD analysis. The CFD analysis was performed in ANSYS CFX which gave a thrust value of 1.49N and 1.09N for S1223 and Clark Y airfoil respectively for the same boundary conditions. The calculation from the Weighted Scoring Method gave the value of 23.406 and 50 for the Clark Y and S1223 airfoil respectively.**

***Keywords*—Altitude, Aerodynamic, Propeller, Thrust, Angle of Attack**

I. INTRODUCTION

UNMANNED Aerial Vehicle refers to an aircraft that operates without a human pilot on board and can be controlled remotely or fly autonomously. UAVs have become essential tools in various industries, including search and rescue (SAR) operations [1]. They have revolutionized the field of search and rescue (SAR), offering unprecedented capabilities for efficient and timely aerial assistance [2]. Their ability to provide real-time data from remote and inaccessible locations has made them indispensable in emergencies. One critical aspect of UAV performance is the propeller, which plays a significant role in the efficiency and effectiveness of these aircraft during operations. Propellers are vital components that enable UAVs to generate thrust and maneuver in different operational environments [3]. Specifically, for high-altitude SAR missions, where thin air and challenging conditions prevail, propeller design becomes paramount to ensure optimal performance and reliability. The commercially available unmanned aerial vehicles are not good enough for search and rescue flights at high altitudes because as the altitude increases, the density of air decreases which affects the thrust generation of the UAV [4]. The relationship between the air density and the altitude is given by equation (1) where ρ is density of air, T_b is standard temperature, L_b is standard temperature lapse rate, h is height above sea level, h_b is reference height, R is universal gas constant, g_o is gravitational acceleration, M is molar mass of Earth's air [5].

$$\rho = \rho_b \left[\frac{T_b - (h - h_b)L_b}{T_b}\right]^{\left(\frac{g_o M}{R * L_b} - 1\right)} \quad (1)$$

When the propeller operates at high altitudes, the power and torque decrease due to the decrease in intake air affected by a decrease in air density and air Reynolds number, which directly affects flight performance parameters of the UAV including propeller efficiency, speed, climbing rate, and maximum range [6]. The maximum flight altitudes which have been achieved using propeller driven aircraft are 20.4km on a combustion driven aircraft (Condor) and 21.3 km for solar electric aircraft (Pathfinder) [7]. A number of airship configurations for high-altitude long-endurance airships have been studied by both government and private organizations. These designs range from conventional cylindrical shapes to spherical or saucer shaped vehicles like Lockheed's high altitude airship concept [8]. Morgado and Abdollahzadeh had designed and analyzed two different propellers for application on MAAT high altitude cruiser airship. The propeller designed with the concept of maximum $L^{3/2}/D$ generates bigger pressure differences between upper and lower surfaces with less friction which mean more thrust than the blade designed with the concept of maximum L/D [7]. Dahal et al. designed the thrust optimized blade for an altitude range of 3,000–5,000 m with a density of air 0.7364 kg/m^3, respectively, and perform thrust analysis. The CFD

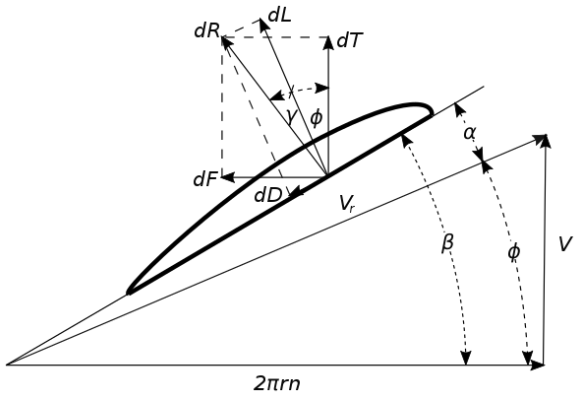

Fig. 1. Velocity vector diagram.

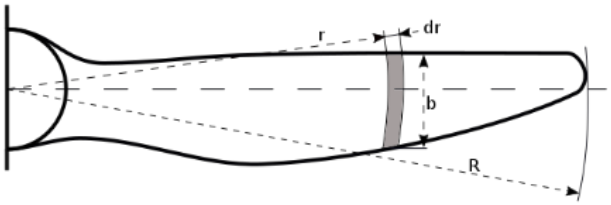

Fig. 2. Propeller top view.

analysis in ANSYS CFX gave a thrust value of 2.27 N whereas the analytical solution gives 1.7 N with 85.6% efficiency [9].

You et al. designed the propeller for a solar unmanned aerial vehicle UAV at 22km altitude and achieved 72% efficiency and 7 N thrust, with 0.5588m diameter propeller rotating at 5500rpm under freestream velocity 50m/s [10]. Singh et al. optimized the AF300 airfoil from existing low Reynolds number airfoils through Xfoil code and compared with other low Reynolds number airfoils suited for small wind turbine rotor blades at Re = 55,000, 100,000 and 148,000, the AF300 airfoil showed good aerodynamic performance attaining the highest combinations of optimum CL and L/D ratios [11]. For axial flight, changing the drag by 25% influence less than 1% on the propeller efficiency. For the hover performance changing the drag by 25% changes the figure of-merit by 3% or less. This demonstrates the low impact of airfoil drag characteristics [12].

Rescuing missing tourists in the remote Himalayas of Nepal poses significant challenges for authorities. They have to navigate the terrain either by helicopter or on foot due to the inaccessibility of many areas [13]. Since the density of air is very low at high altitudes, the search and rescue mission becomes difficult by a normal UAV. Thousands of individuals residing in remote regions of Nepal lack access to adequate healthcare facilities and have to travel long journeys on foot if they become unwell. The drone designed, fabricated and assembled by the innovative young college graduates in the National Innovation Centre (NIC) can only carry a one kg load about two km, but the team is working on improving the range so it can carry a heavier load over a longer distance [14]. Due to the increasing number of Nepalese and foreigners who trek up into the remote wilderness and high altitudes, Himalayan Rescue Association Nepal (HRA) is formed in 1973 with an objective to reduce casualties in the Nepal Himalayas [15]. Hence, this research is done for analysis and comparison of Unmanned Aerial Vehicle's propellers for search and rescue mission.

II. Materials and Methods

The method of this research is based on a field study. The main objective of this research is to analyze and compare the UAV propellers for high-altitude search and rescue missions. The majority of unmanned aerial vehicles (UAVs) are equipped with fixed-pitch propellers [16, 17]. Various theories, such as blade element theory, vortex theory [18], momentum theory [19, 20], flat plate theory [21], and semiempirical methods [22], have been proposed to predict the efficiency of fixed-pitch propellers. Blade element theory is simple and it accounts for the Reynolds number effects in low advance ratios [23, 24, 25]. Hence, the blade element theory is widely used to model propeller blade aerodynamics.

A. Simple Blade Element Theory

It was used for analytically calculating the lift force created by propellers. While for the numerical calculation, Xflr5 was used for the airfoil selection by determining the lift and drag coefficient of propellers at low Reynolds Numbers, SolidWorks software was used in the 3D modelling of S1223 and Clark-Y Airfoils and ANSYS was used for the determination of the Lift and Drag force produced by the propellers. And for experimental verification bench-test setup was equipped at different altitudes. The total thrust, torque and the efficiency of the propeller having B number of blades are given by equations (2), (3) and (4) respectively [26, 27, 28], where ρ is the air density, V is the velocity, b is the chord length, r is the radius of the blade, B is the number of blades, C_L is the coefficient of lift, γ is the angle between the lift component and the resultant force, $\emptyset$ is the angle between the direction of motion of the element and the plane of rotation, and β is the blade angle. Fig. 1 shows the velocity vector diagram with reactions in the blade and Fig. 2 shows the propeller top view [29].

$$F_t = \int_0^r \frac{1}{2}\rho V^2 b dr B C_L \frac{\cos(\gamma+\emptyset)}{\cos(\gamma)\sin^2(\emptyset)} \quad (2)$$

$$Q = \int_0^r \frac{1}{2}\rho V^2 br dr B C_L \frac{\sin(\gamma+\emptyset)}{\sin(\gamma)\cos^2(\emptyset)} \quad (3)$$

$$\eta = \frac{F_t V}{2\pi n Q} \quad (4)$$

$$V_{max} = \sqrt{{V_\infty}^2 + (\pi N D)^2} \quad (5)$$

The blade tip speed is given by equation (5) and due to high noise levels, the values are limited to 250 m/s. Where V_{max} is the resultant motion velocity, V∞ is the translatory speed, N is the rotational speed and D is the diameter of the propeller. For

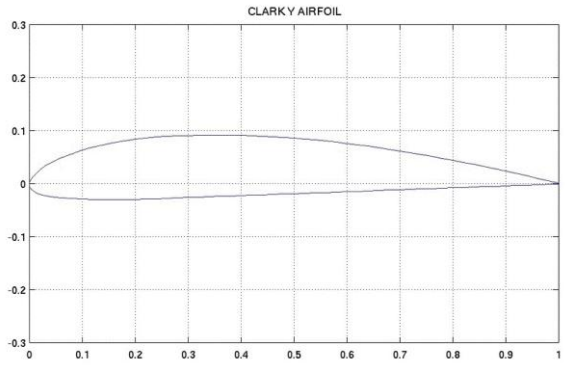

Fig. 3. Clark-Y airfoil.

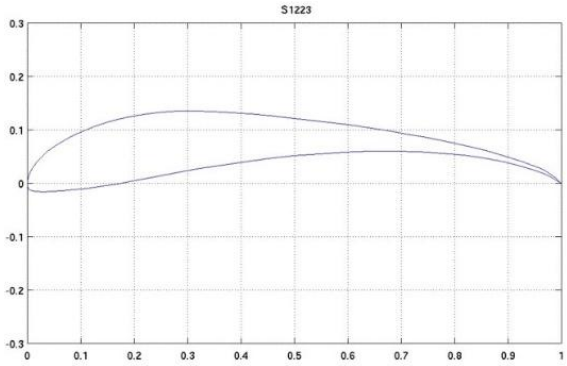

Fig. 4. S1223 airfoil.

the selection of the best airfoil, the drag and lift coefficient of different airfoils was analyzed.

$$b = (0.08424 - 0.08579r + 4.7176r^2 - 9.6225r^3 + 8.5004r^4 - 2.7959r^5)D \quad (6)$$

Analytical thrust calculation was based on equation (1); Assumed parameters are the density of air at 3610m is 0.8194 kg/m^3, the number of blades is 2, C_l and C_d for S1223 at AOA 4° is 1.35 and 0.05, C_l and C_d for Clark-Y at same AOA are 0.75 and 0.06, the radius of the blade is 0.15 m, and the chord is given by equation (6) [30]. Airfoil designs of Clark-Y and S1223 are shown in the Figs. 3 and 4 [31,32].

B. Xflr5 Analysis

Xflr5 is an analysis tool for airfoils and wings operating at low Reynolds Numbers. The value of lift and drag coefficient were analyzed for the propellers in XFLR5 software under operating conditions. The value of Reynold's number was calculated from equation (7) [33].

$$\mathrm{Re} = \frac{\rho L v}{\mu} \quad (7)$$

where, ρ = density of air = 0.821kg/m^3, L = 25.4 cm, v = velocity of flight =10 m/s and $\mu = 1.6 \times 10^{-5}$ m^2/s. The analysis was done in the XFLR5 software to determine the effect of AOA on the coefficient of lift and drag for the Clark Y and

TABLE I: WEIGHTED SCORE FOR VARIOUS PARAMETERS

Parameter	Evaluation Criteria	Weighted Score
C_{L_0}	Highest is the best	0.15
C_{l_max}	Highest is the best	0.15
α_{stall}	Highest is the best	0.1
C_{D_min}	Lowest is the best	0.15
C_L/C_{D_max}	Highest is the best	0.15
$C_L^{3/2}/C_D$	Highest is the best	0.15

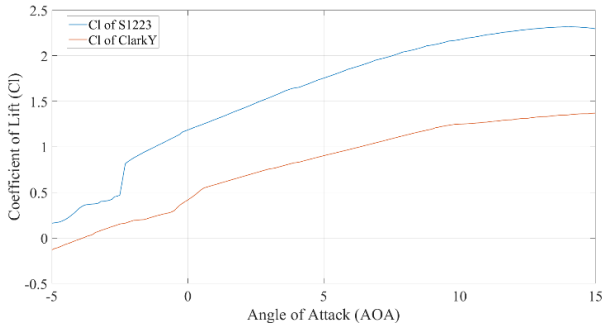

Fig. 5. C_l versus AoA of S1223 and Clark-Y airfoil.

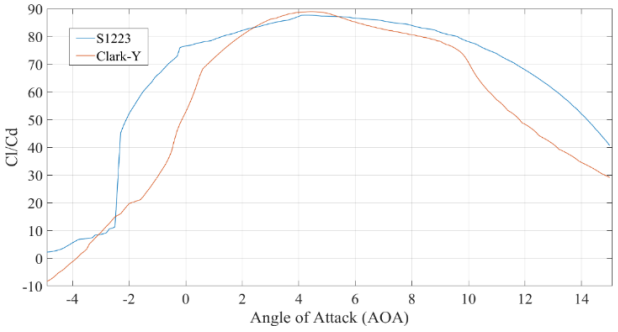

Fig. 6. C_l/C_d vs AoA of S1223 and Clark-Y airfoil.

S1223 airfoil propeller. Figs. 5 and 6 show the effect of AOA on the coefficient of lift and C_l/C_d ratio for the propellers, respectively obtained from Xflr5 software.

C. Weighted Scoring Method (WSM)

A selection method is required to optimize the airfoil selection. The Weighted Scoring Method (WSM) is a selection method comparing multiple criteria, where a set of criteria for the best performance of these two airfoils has to be set to select the best airfoil[34]. It includes determining all the criteria related to the selection, giving each criterion a weighted score to reflect its relative importance, and evaluating each criterion. Here, C_{L_0} is the lift coefficient at an angle of attack equal to 0°, C_{l_max} is the maximum lift coefficient, α_{stall} is the stall angle of attack, C_{D_min} is the minimum drag coefficient, C_L/C_{D_max} is the maximum of the range parameter, and $C_L^{3/2}/C_D$ is the maximum of the endurance parameter. WSM consists of the following steps:

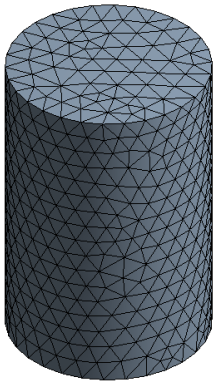

Fig. 7. Static domain for CFD.

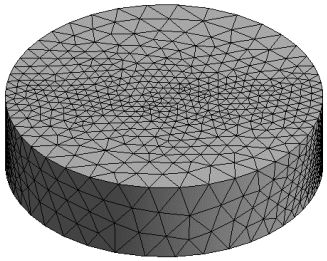

Fig. 8. Rotating domain.

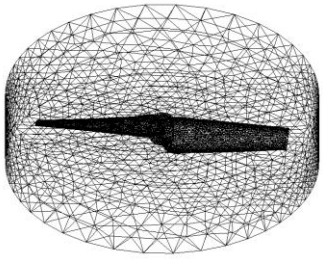

Fig. 9. Wireframe of rotating domain.

1. Determining all the criteria.
2. Distributing to each criterion a weighted score.
3. Evaluating each criterion of an option.
4. Multiplying the points evaluated by the weighted score.
5. Making the sum of all the products and selecting the airfoil with the highest total points.

Obtained score:

For Clark-Y = (0.15×0.4) + (0.15×1.4) + (0.1×15) + (0.15×0.03) + (0.15×89) + (0.15×55.21) = 23.406

For S1223 = (0.15×1.2) + (0.15×2.3) + (0.1×14) + (0.15×0.015) + (0.15×88) + (0.15×232.54) = 50

D. CFD Analysis

1) Computational Model

The computational domain is divided into two parts. The stationary domain takes 8 times the diameter of the propeller in the upstream and downstream. The span-wise diameter is 8 times. Also, the inlet, outlet, and propeller outer region are stationary. The rotating domain with cylindrical shape has a diameter of 450 mm and a height of 450 mm. Figs. 7, 8, and 9

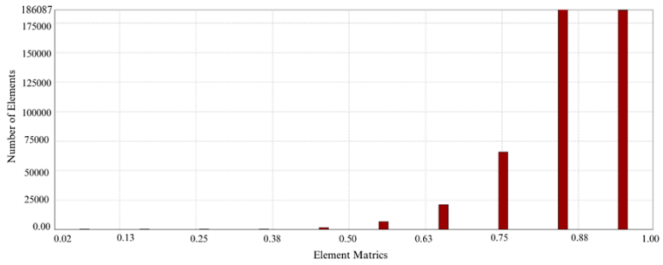

Fig. 10. Orthogonal quality of Clark-Y airfoil.

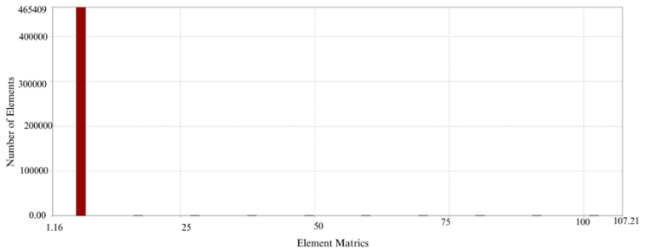

Fig. 11. Aspect ratio of Clark-Y airfoil propeller.

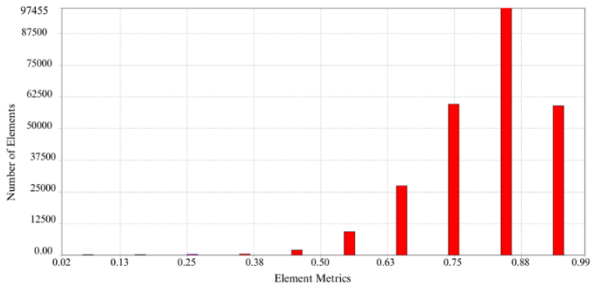

Fig. 12. Orthogonal quality of S1223 airfoil

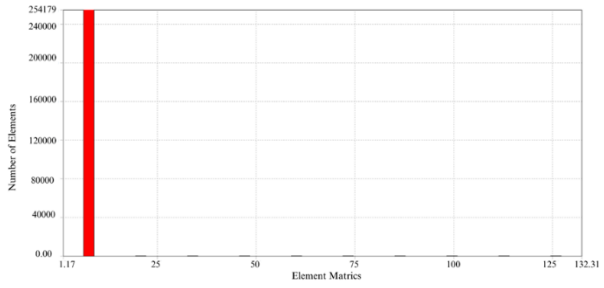

Fig. 13. Aspect ratio of S1223 airfoil propeller

show individual meshes for stationary and rotating domains along with the propeller blade. The number of meshes carried out in the analysis is 465428, which is a fine mesh. The mesh quality is determined by various parameters, one being the element's quality, which is of average of 0.836, and the next is aspect ratio which is in average of 1.84 and third being the orthogonal quality of the mesh which is around 0.86. The figures 10, 11, 12 and 13 show the element's aspect ratio and orthogonal quality for two different propellers.

2) Computational Model

The analysis for the propeller was carried out using ANSYS Fluent, where the propeller is stationary under a rotating coordinate system. K-e standard equation acts as the governing equation while the finite volume methods with the pressure-based solver are used to discretize the governing equations. The

TABLE II: BOUNDARY CONDITIONS

Inlet Boundary Conditions	
Inlet Type	Velocity
Velocity	1 m/s
Wall Boundary Condition	
Wall Motion	Stationary Wall
Shear Boundary Condition	No Slip
Outlet Boundary Condition	
Outlet Type	Pressure Outlet
Guage Pressure	0 MPa
Properties of the flowing fluid	
Fluid	Air at 25°C
Density	0.821 Kg/m^3

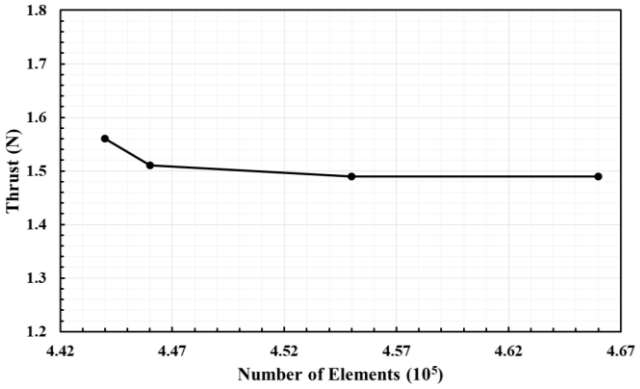

Fig. 14. Mesh independence test for S1223 airfoil.

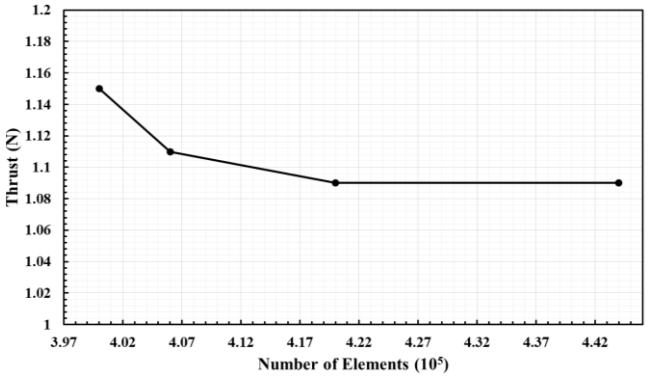

Fig. 15. Mesh independence test for Clark-Y

convergence is also guaranteed by monitoring the residual value drops below 1.0×10^{-3}.

3) Boundary Conditions

All the boundary conditions are applied based on the experiment carried out at an altitude of 3610 m. The flowing fluid is considered as air at 25°c and the flow is transient with the time step size of 0.00015s. The boundary conditions used in the Fluent Analysis are shown in Table 2.

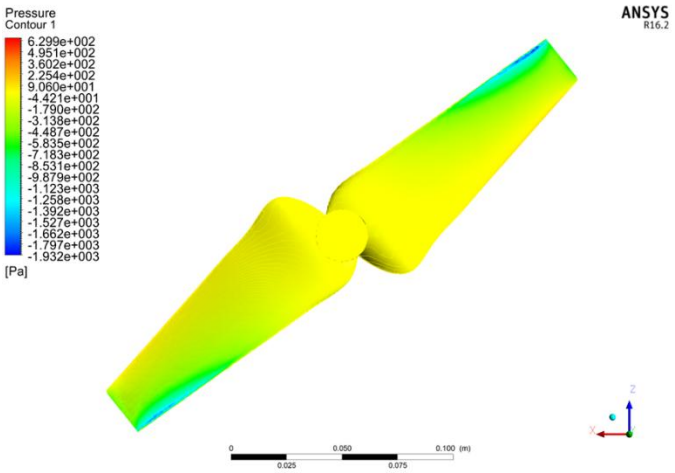

Fig. 16. Pressure contour for Clark-Y airfoil suction side.

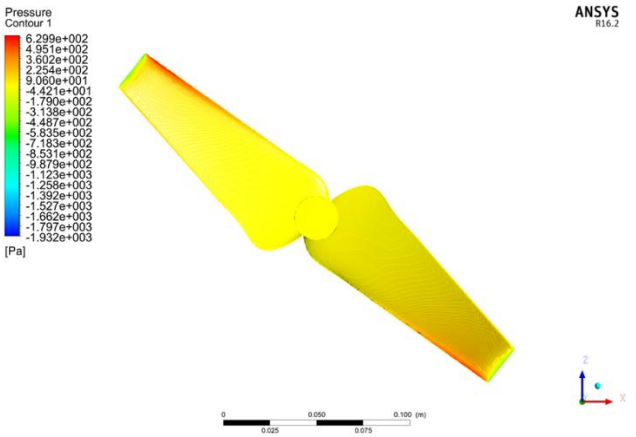

Fig. 17. Pressure contour for Clark-Y airfoil pressure side.

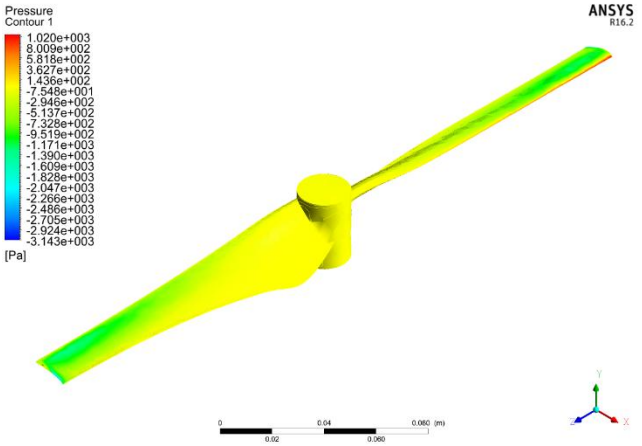

Fig. 18. Pressure contour of S1223 airfoil suction side.

4) Mesh Independence Test

The mesh independence test is done, which is the crucial step in ensuring the accuracy and reliability of the result. The mesh independence test supported the results of independence at the

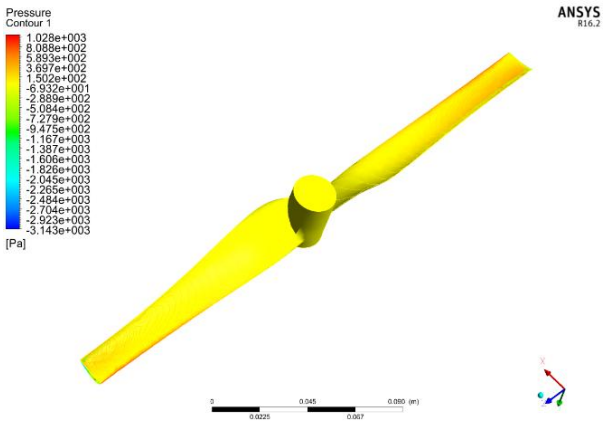

Fig. 19. Pressure contour of S1223 airfoil propeller pressure side.

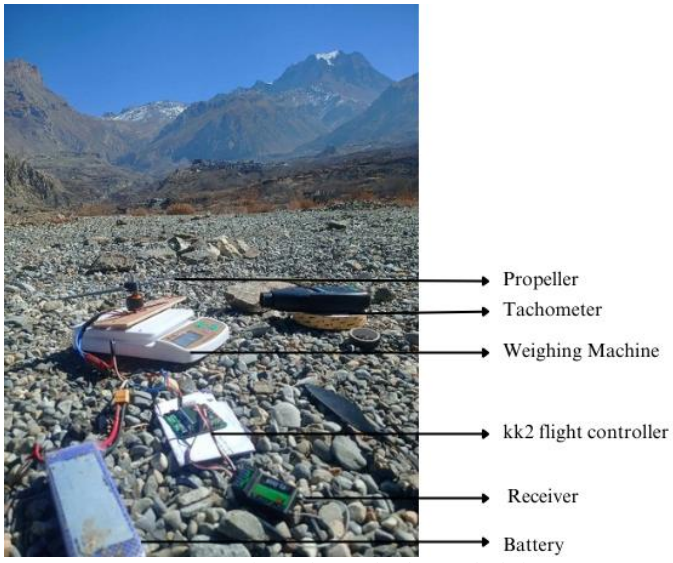

Fig. 20. Experimental setup for thrust calculation.

rpm of 3000 rpm. The graph for the mesh independence test is attached in the Figs. 14 and 15 for S1223 and Clark-Y airfoil, respectively.

5) Mesh Independence Test

The pressure contours, as seen in Figs. 16, 17, 18, and 19 show the pressure distribution profile for the Clark Y and S1223 airfoil propeller. For the Clark-Y propeller, the blade faced the highest pressure of 629.9 Pa at the pressure side and the lowest pressure of -1932 Pa at the suction side. For S1223 Airfoil Propeller, the blade faced the highest pressure of 1020 Pa at the pressure side and the lowest pressure of -3143 Pa at the suction side.

6) Manufacturing and Testing

The designed blades were 3D printed first, and simple filling was performed to improve the surface finish of the propellers. The printed propellers were tested at different altitudes, including 1190m, 2437m, 2730m, 3519m, and 3610m. The route for various altitudes was from Pokhara (822m) to Muktinath (3610m), and the thrust calculations were done in between these altitudes. Before the final thrust test, a static balance check was performed. The thrust testbed can be seen in Fig. 20. A digital tachometer was used to measure the rotational velocity of the propeller, and an electronic speed controller was used to change the rotational speed of the propeller. Due to the testbed limitations, a higher RPM could not be tested. Figs. 21 and 22 show the variation of experimental thrust generations at the various altitudes with the rotational speed of the propellers. It can be seen from the graph that as the altitude increases, the thrust generated by the propellers decreases and vice versa.

TABLE III: COMPARISON OF ANALYTICAL, NUMERICAL AND EXPERIMENTAL VALUES

Airfoil	Altitude	Analysis	Numeric	Experiment	RPM
Clark Y	3610 m	0.6 N	1.09 N	0.42 N	3000
S1223	3610 m	1.45 N	1.49 N	0.63 N	3000

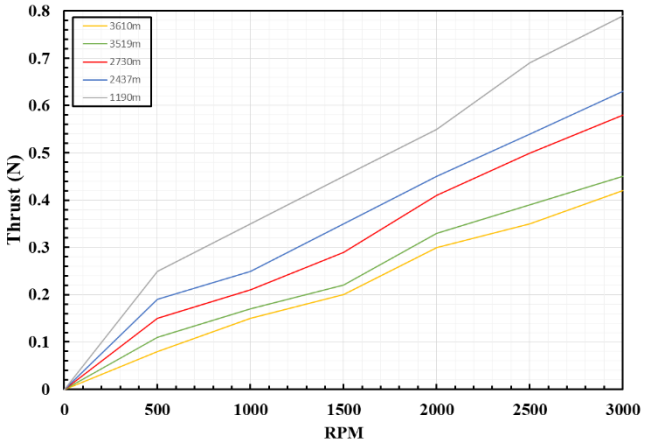

Fig. 21. Result of experimental testing of Clark-Y.

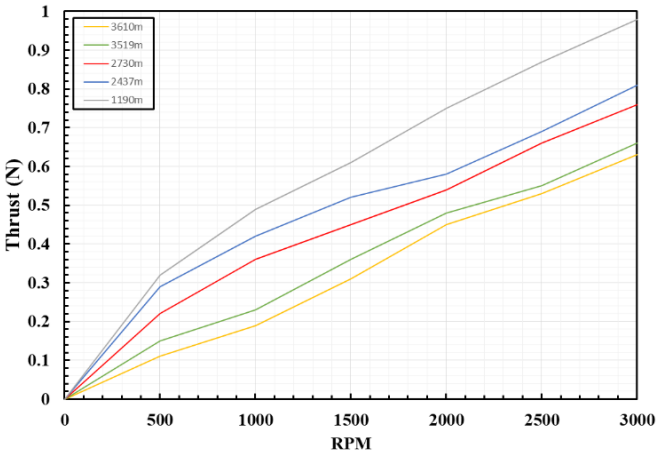

Fig. 22. Result of experimental testing of S1223.

III. RESULTS AND DISCUSSION

The results obtained from analytical values, experimental values and numerical values have been compared in Table 3. Experimental analysis of the blade gave a thrust of 0.63 N and 0.42 N for the S1223 airfoil and Clark Y, respectively, at 3000 RPM at

3610 m. The analytical solution for thrust with the same conditions was 1.45 N and 0.6 N for the S1223 airfoil and the Clark Y, respectively. The validation of experimental results was done by the CFD analysis. The CFD analysis was performed in ANSYS Fluent, which gave a thrust value of 1.49 N and 1.09 N for the S1223 airfoil and Clark Y, respectively, for the same boundary conditions. The calculation from the Weighted Scoring Method gives the value of 23.406 and 50 for the Clark Y and S1223 airfoils, respectively. Thus, the result suggests that the S1223 airfoil is better than the Clark Y for search and rescue flight at high altitudes. There is a variation in the analytical values, experimental values, and numerical values. This could be due to various factors involved in the experiment, like the aerodynamics profile of the fabricated propeller may not be accurately the same as the designed propeller.

V. Conclusion

The design, simulation and analysis of the UAV propellers were done in XFLR5, SOLIDWORKS, and ANSYS. The results obtained were compared and verified and found to be close to each other. The blades were designed for an altitude range of 3,000m to 5,000m, which is suitable for search and rescue operations in Nepal. The blade was tested at high altitude, ranging from 1190m to 3610m and their corresponding thrust were calculated. These are the conclusions that can be drawn from the research work.

i) The CFD thrust analysis gave thrust generation of 1.49 N and 1.09 N for S1223 airfoil and Clark Y, respectively, for an altitude of 3600 m with a rotational velocity of 3000 RPM.

ii) The analysis gave the thrust generation of 1.45 N and 0.6 N for S1223 airfoil and Clark Y, respectively, for an altitude of 3600 m with a rotational velocity of 3000 RPM.

iii) The experimental analysis gave the thrust of 0.63 N and 0.42 N for S1223 airfoil and Clark Y, respectively, for an altitude of 3600 m with a rotational velocity of 3000 RPM.

iv) The calculation from the Weighted Scoring Method gives the value of 23.406 and 50 for the Clark Y and S1223 airfoil, respectively. Thus, the result suggests that the S1223 airfoil is better than the Clark Y for search and rescue flight at high altitudes.

References

[1] S. A. H. Mohsan, N. Q. H. Othman, Y. Li, M. H. Alsharif, and M. A. Khan, "Unmanned aerial vehicles (UAVs): practical aspects, applications, open challenges, security issues, and future trends," *Intell. Serv. Robot.*, vol. 16, no. 1, pp. 109–137, 2023.

[2] "Remote Sensing | Free Full-Text | Unmanned Aerial Vehicles for Search and Rescue: A Survey." Accessed: Feb. 03, 2024. [Online]. Available: https://www.mdpi.com/2072-4292/15/13/3266

[3] A. Sawale, D. Archana, and C. Seshank, "Design and Analysis of Propeller," *IOP Conf. Ser. Mater. Sci. Eng.*, vol. 455, p. 012018, Dec. 2018, doi: 10.1088/1757-899X/455/1/012018.

[4] H. Ding, R. Liu, Z. Zhang, C. Yang, Y. Jiao, and L. Hu, *Study on the Influence of High-altitude on Performance of an Opposed-Piston Gasoline Engine*. 2020, p. 171. doi: 10.1109/IPEC49694.2020.9115160.

[5] K. Fea, "Determination of the Density of Air at an Altitude of 3,500 km," *Nature*, vol. 205, no. 4969, pp. 379–381, Jan. 1965, doi: 10.1038/205379a0.

[6] R. Liu, Z. Zhang, Y. Jiao, C. Yang, and W. Zhang, "Study on Flight Performance of Propeller-Driven UAV," *Int. J. Aerosp. Eng.*, vol. 2019, p. e6282451, Apr. 2019, doi: 10.1155/2019/6282451.

[7] J. Morgado, M. Abdollahzadeh, M. A. R. Silvestre, and J. C. Páscoa, "High altitude propeller design and analysis," *Aerosp. Sci. Technol.*, vol. 45, pp. 398–407, Sep. 2015, doi: 10.1016/j.ast.2015.06.011.

[8] A. Colozza, A. Corporation, B. Park, and J. L. Dolce, "High-Altitude, Long-Endurance Airships for Coastal Surveillance," 2005.

[9] C. Dahal, H. Dura, and L. Poudel, "Design and Analysis of Propeller for High Altitude Search and Rescue Unmanned Aerial Vehicle," *Int. J. Aerosp. Eng.*, vol. 2021, p. 13, Jan. 2021, doi: 10.1155/2021/6629489.

[10] K. You, X. Zhao, S.-Z. Zhao, and M. Faisal, "Design and Optimization of a High-altitude Long Endurance UAV Propeller," *IOP Conf. Ser. Mater. Sci. Eng.*, vol. 926, no. 1, p. 012018, Sep. 2020, doi: 10.1088/1757-899X/926/1/012018.

[11] R. K. Singh, M. R. Ahmed, M. A. Zullah, and Y.-H. Lee, "Design of a low Reynolds number airfoil for small horizontal axis wind turbines," *Renew. Energy*, vol. 42, pp. 66–76, Jun. 2012, doi: 10.1016/j.renene.2011.09.014.

[12] O. Gur, "AIRFOIL IMPORTANCE FOR PROPELLER OPTIMIZED DESIGN," Mar. 2022.

[13] P. Gyawali and C. Dahal, "Using a GPS enabled body area network (BAN) based health tracker, that uses GSM, for mountaineers in Nepal," in *International Astronautical Congress*, 2018, p. 6.

[14] G. Sharma, Nepal's medical drones bring healthcare to the Himalayas. Accessed: Apr. 30, 2018. [Online]. Available: https://www.reuters.com/article/idUSKBN1I114F/

[15] B. Basnyat and G. Bashyal, "Nepali Times," High Himalayan rescue. Accessed: May 26, 2023. [Online]. Available: https://nepalitimes.com/opinion/comment/high-himalayan-rescue

[16] R. Glassock, J. Hung, L. Gonzalez, and R. Walker, "Design, Modelling and Measurement of Hybrid Powerplant for Unmanned Aerial Systems (UAS)," *Aust. J. Mech. Eng.*, vol. 6, Jan. 2007, doi: 10.1080/14484846.2008.11464559.

[17] E. Torenbeek and H. Wittenberg, Eds., "Aeroplane Performance," in *Flight Physics: Essentials of Aeronautical Disciplines and Technology, with Historical Notes*, Dordrecht: Springer Netherlands, 2009, pp. 253–325. doi: 10.1007/978-1-4020-8664-9_6.

[18] "Validation of Vortex Propeller Theory for UAV Design with Uncertainty Analysis | Aerospace Sciences Meetings." Accessed: Apr. 22, 2024. [Online]. Available: https://arc.aiaa.org/doi/abs/10.2514/6.2008-406

[19] "Propeller Momentum Theory with Slipstream Rotation | Journal of Aircraft." Accessed: Apr. 22, 2024. [Online]. Available: https://arc.aiaa.org/doi/abs/10.2514/2.2914?journalCode=ja

[20] M. K. Rwigema, "Propeller blade element momentum theory with vortex wake deflection," in *27th International congress of the aeronautical sciences*, 2010, pp. 727–735. Accessed: Apr. 22, 2024. [Online]. Available: http://www.icas.org/ICAS_ARCHIVE/ICAS2010/PAPERS/434.PDF

[21] "Fixed pitch rotor performance of large horizontal axis wind turbines - NASA Technical Reports Server (NTRS)." Accessed: Apr. 22, 2024. [Online]. Available: https://ntrs.nasa.gov/citations/19830010962

[22] B. Montgomerie, "Methods for root effects, tip effects and extending the angle of attack range to {+-} 180 deg., with application to aerodynamics for blades on wind turbines and propellers," Jun. 2004, Accessed: Apr. 22, 2024. [Online]. Available: https://www.osti.gov/etdeweb/biblio/20607079

[23] "Validation of New Formulations for Propeller Analysis | Journal of Propulsion and Power." Accessed: Apr. 22, 2024. [Online]. Available: https://arc.aiaa.org/doi/abs/10.2514/1.B35240

[24] M. Ol, C. Zeune, and M. Logan, "Analytical/Experimental Comparison for Small Electric Unmanned Air Vehicle Propellers," in *26th AIAA Applied Aerodynamics Conference*, American Institute of Aeronautics and Astronautics. doi: 10.2514/6.2008-7345.

[25] M. McCrink and J. W. Gregory, "Blade Element Momentum Modeling of Low Small UAS Electric Propulsion Systems," in *33rd AIAA Applied Aerodynamics Conference*, American Institute of Aeronautics and Astronautics. doi: 10.2514/6.2015-3296.

[26] A. Dumitrache, M. Pricop, M. Niculescu, M. G. Cojocaru, and T. Ionescu, "DESIGN AND ANALYSIS METHODS FOR UAV ROTOR BLADES," *Sci. Res. Educ. AIR FORCE*, vol. 19, pp. 115–126, Jul. 2017, doi: 10.19062/2247-3173.2017.19.1.48.

[27] "Elements of propeller and helicopter aerodynamics | CiNii Research." Accessed: Apr. 22, 2024. [Online]. Available: https://cir.nii.ac.jp/crid/1130000798151837440

[28] "AircraftPropellerDesign1930.pdf." Accessed: Feb. 06, 2024. [Online]. Available:https://ia801408.us.archive.org/25/items/AircraftPropellerDesign1930/AircraftPropellerDesign1930.pdf

[29] R. Dasilveira, "Optimum Propeller Designs for Electric UAVs," *Auburn Univ.*, 2002.

[30] "Performance Calculation and Design of Stratospheric Propeller | IEEE Journals & Magazine | IEEE Xplore." Accessed: Apr. 22, 2024. [Online]. Available: https://ieeexplore.ieee.org/abstract/document/7982612/

[31] E. P. Hartman and D. Biermann, "The Aerodynamic Characteristics of Full-Scale Propellers Having 2, 3, and 4 Blades of Clark Y and R.A.F. 6 Airfoil Sections." Jan. 01, 1938. Accessed: May 25, 2024. [Online]. Available: https://ntrs.nasa.gov/citations/19930091715

[32] P. Sonwane, M. Yadav, N. Bunker, S. Sonwane, and V. Shirsath, "Economical Design Perspective for Aircraft by Optimizing Airfoil S1223," *E-Prime - Adv. Electr. Eng. Electron. Energy*, vol. 8, p. 100531, Jun. 2024, doi: 10.1016/j.prime.2024.100531.

[33] "Low-Reynolds-Number Airfoils | Annual Reviews." Accessed: Apr. 22, 2024. [Online]. Available: https://www.annualreviews.org/content/journals/10.1146/annurev.fl.15.010183.001255

[34] A. Jadhav and R. Sonar, "Analytic hierarchy process (AHP), weighted scoring method (WSM), and hybrid knowledge based system (HKBS) for software selection: a comparative study," in *2009 Second International Conference on Emerging Trends in Engineering & Technology*, IEEE, 2009, pp. 991–997. Accessed: Apr. 22, 2024. [Online]. Available: https://ieeexplore.ieee.org/abstract/document/5395484/